forum acusticum 2026
8-12 September · Graz, Austria

NUMERICAL SIMULATION AND EVALUATION OF VISCOUS EFFECTS IN A COUPLED MODULATED ULTRASOUND MICROSPEAKER

Tobias Wilczacki[1], Dominik Mayrhofer[1], Manfred Kaltenbacher[1]
[1] *Graz University of Technology, Inffeldgasse 18/I, 8010 Graz, Austria*

This contribution has been accepted based on the submitted abstract. The submitted manuscript was not reviewed and is reproduced here without edits or corrections by the conference board. Neither the EAA nor the AAA take responsibility for its contents.

Abstract

Research on modulated ultrasound microspeakers has been increasing steadily in recent years, with new modulation and actuation techniques being proposed. Such devices are highly integrated, often consisting of multiple moving parts and varying channel widths that require complex simulation to accurately model their behavior. This makes accurate simulations very challenging. In this contribution, we present a fully coupled multiphysics finite element model of a microspeaker comprising two moving membranes, a pressure chamber between them, and air channels with varying acoustic impedance. Incorporating electrostatic actuation, nonlinear membrane mechanics and a viscous air domain, the model aims to accurately capture surface traction and squeeze-film damping effects. Using a frequency-modulated excitation, the modulation behavior is investigated. In the spectrum of the resulting modulated ultrasound pressure signal, the low-frequency audio signal components are present, confirming the expected modulation behavior. Initial results indicate an increase in total harmonic distortion when nonlinear and viscous effects are included compared to a linear model. This provides crucial insight into the device's development and demonstrates the importance of a fully coupled simulation for predicting the modulation behavior. All steps, from modeling and meshing to the coupled simulation, were done using only open-source software (*Gmsh*, *openCFS*), providing a reproducible framework for simulation of highly coupled systems.

Keywords: *viscous effects, FEM, ultrasound, microspeaker*

Corresponding author: *wilczacki@tugraz.at.*

1. Introduction

As research and development of electrostatic-driven modulated-ultrasound speakers have gained traction in recent years [1], [2], [3], [4], [5], new state-of-the-art designs have been proposed and tested to increase efficiency and reduce footprint and power consumption. Modulated ultrasound loudspeakers feature a driving unit as well as a shutter/demodulater which are used to produce sound in the audible frequency range from 20 Hz to 20 by demodulating an ultrasound carrier signal. For effective demodulation, the actuator undergoes comparatively large deformations, which also introduces challenges in the modeling process due to the necessity to incorporate domain movement and non-linearities. To retain all necessary effects, highly coupled multiphysical finite element simulations are the go-to way to investigate such designs and modulation methods. Additionally, network models can serve as a fast but usually less accurate way to speed up design choices [4]. Nevertheless, it is important to validate such network models with simulation and experiments. One downside for the scientific space is the reproducibility of such simulations, as most closed-source software comes with major licensing costs. Open-source tools reduce costs and also increase transparency, enabling researchers to share their models, code, and data openly. In this investigation, an electrostatic-driven modulated-ultrasound speaker similar to the one proposed by SonicEdge in [4] is modeled using *Gmsh* [6] and simulated using the open-source multiphysics FEM solver *openCFS* [7].

2. Model description

The model is constructed based on the geometry of an existing microspeaker array depicted in Fig. 1. Due to the symmetric design of the microcell, only one-third of the structure is modeled, with the corresponding symmetry boundary conditions applied. One further symmetry was not implemented, as further reduction introduced complications during the

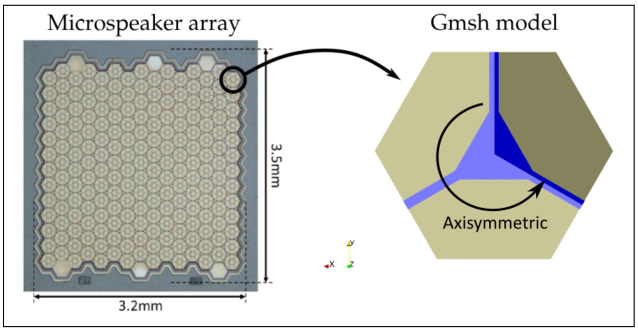

Figure 1: Top view of the existing microspeaker array and top view of the *Gmsh* used for the simulation depicting the axisymmetry used to reduce complexity

meshing process and the current model was already suitable for simulation. Each microcell in the array consists of three membranes stacked on top of each other. The schematic of the stacked membranes can be seen in Fig. 2.

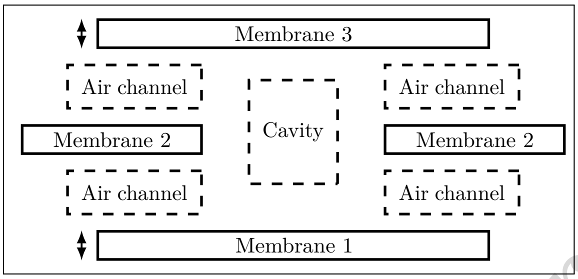

Figure 2: Schematic side view of the microspeaker with three membranes stacked horizontally, the cavity created between them and the air channels

The microcell model consists of membranes stacked horizontally. The two outer membranes, membranes 1 and 3, are movable and are actuated electrostatically. The middle membrane, membrane 2, is fixed at the outer edges, acts as a ground plane for the outer membranes, and creates a middle cavity. In the overlap regions between the membranes, air channels with varying gaps are created. Those air channels are used for demodulating the modulated ultrasound signal. At the outer edges the membranes are fixed in place. The resulting 3D model of the membranes is depicted in Fig. 3.

The mechanical model is then embedded in a viscous air domain that acts as the main damping force of the membranes and thus includes the viscous effects of air present at such high actuation frequencies. To reduce computational complexity, the viscous air domain is switched to a purely acoustic domain as soon as viscous effects can be neglected [8]. In this domain, the radiated sound pressure is measured at a distance of four times the micro speaker diameter.

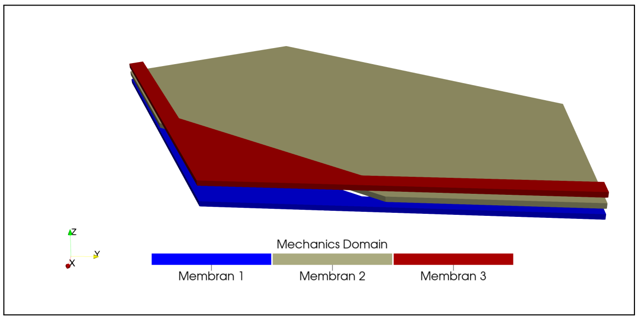

Figure 3: 3D model of the mechanical domain used for the simulation

3. Excitation and modulation

As an excitation, a simple frequency modulation setup is used [3]. The modulation signal is produced by membrane 3. The carrier signal is produced by membrane 1. Equations (1) and (2) state the excitation voltage applied to the corresponding membranes.

$$U_{\mathrm{mb1}}(t) = U_{\mathrm{max}} \sin(2\pi\, t\, f_{\mathrm{carrier}}) \tag{1}$$
$$U_{\mathrm{mb3}}(t) = U_{\mathrm{max}} \sin(2\pi\, t\, (f_{\mathrm{carrier}} - f_{\mathrm{audio}})) \tag{2}$$

Here, the carrier frequency $f_{\mathrm{carrier}} = 400\,\mathrm{kHz}$, the audio signal is set to $f_{\mathrm{carrier}} = 40\,\mathrm{kHz}$ and the maximum voltage has been chosen such that the residual gap between the membranes is close to 50 % of the original gap. With this setup, the two signals are intermodulated in the viscous air domain between the membranes. The varying air channels acting as an impedance modulation demodulate the resulting pressure signal, and the low-frequency audio signal is produced. It has to be noted that the low-frequency signal is still in the ultrasound range and was solely chosen to reduce computation time. The workflow can be applied to any audio frequency, but the lower the audio frequency, the longer the computation time.

4. Governing Equations

The microspeaker model consists of an excitation that is defined by the electrostatic force acting on the membranes. A voltage is applied to the top and bottom membranes. The middle membrane is set to ground. To calculate the electrostatic force the electrostatic partial differential equation (PDE), (3), is used. This PDE describes the electrostatic field by the divergence of the gradient of the electrostatic scalar potential ϕ scaled by the permittivity ϵ.

$$-\nabla \cdot \epsilon \nabla \phi = 0 \tag{3}$$

The excitation voltages are directly prescribed via inhomogeneous Dirichlet boundary conditions onto the surfaces of the membranes by setting $\phi(t) = U_{\mathrm{mb1}}(t)$ for membrane 1, $\phi(t) = 0$ for membrane 2 and $\phi(t) = U_{\mathrm{mb3}}(t)$ for membrane 3 at the boundary. The resulting electrostatic force is then applied to the mechanical model of the microspeaker by coupling the electrostatic force as a boundary condition to the mechanics PDE, (4).

$$\rho \boldsymbol{f} + \nabla \cdot [\boldsymbol{\sigma}] = \rho \frac{\partial^2 \boldsymbol{u}}{\partial t^2} \tag{4}$$

This PDE balances the forces acting on a body, the volume forces given by the force density $\boldsymbol{f}$ times the density ρ and the surface forces, defined by the divergence of the stress tensor $[\boldsymbol{\sigma}]$ with the forces acting an a body described by Newtons second law, acceleration $\frac{\partial^2 \boldsymbol{u}}{\partial t^2}$ times the density ρ. This PDE is then solved for the membrane displacement $\boldsymbol{u}$ according to the material parameters and the boundary conditions. For the nonlinear case, the mechanics PDE is solved iteratively with the internal forces, given by $\nabla \cdot [\boldsymbol{\sigma}]$, being dependent on the displacement. The outward-facing surfaces of the membranes are fixed in place by using the homogeneous Dirichlet boundary condition, setting the displacement to zero for all directions. This results in the membranes being clamped at the outer edges. Around the membranes, the air is modeled using the linearized compressible flow equations (LinFlow PDE), (6) and (7), to include viscous effects. As this domain moves with the membranes, the displacement solved for in the mechanics PDE has to be incorporated into the LinFlow PDE via grid movement. This adaptation is done using the smooth PDE, 5, a quasi-mechanical modeling that adapts the grid according to a quasi-stiffness. This approach was introduced in [8]. A linearized Ansatz for the strain, $\frac{1}{2}(\nabla \boldsymbol{u} + \nabla \boldsymbol{u}^{\mathrm{T}})$), only depending on the displacement $\boldsymbol{u}$, is used. The resulting displacement is therefore only dependent on the stiffness tensor $[\boldsymbol{C}]$. The displacement at the membrane surfaces is prescribed as an inhomogeneous Dirichlet boundary condition in the smooth PDE that is used to update the grid in the LinFlow domain.

$$-\nabla \cdot \left([\boldsymbol{C}] : \frac{1}{2}(\nabla \boldsymbol{u} + \nabla \boldsymbol{u}^{\mathrm{T}}) \right) = 0 \tag{5}$$

The velocity at the membrane edges is then coupled to the LinFlow PDE as a boundary condition. This PDE is then solved on the updated grid. To include the viscous air damping, the surface traction at the membrane surfaces is calculated and is then iteratively coupled back to the mechanics PDE.

$$\frac{1}{c^2}\frac{\partial p}{\partial t} + \rho_0 \nabla \cdot \boldsymbol{v} - \frac{1}{c^2} \boldsymbol{v}_{\mathrm{grid}} \cdot \nabla p = 0 \tag{6}$$

$$\rho_0 \frac{\partial \boldsymbol{v}}{\partial t} - \rho_0 \boldsymbol{v}_{\mathrm{grid}} \cdot \nabla \boldsymbol{v} = \nabla \cdot [\boldsymbol{\sigma}_{\mathrm{f}}] \tag{7}$$

In these equations, p denotes the perturbed pressure, $\boldsymbol{v}$ the velocity of the medium, c the speed of sound, t the time, ρ_0 the mean density, $\boldsymbol{v}_{\mathrm{grid}}$ the grid velocity and $[\boldsymbol{\sigma}_{\mathrm{f}}]$ the viscous stress tensor. In the simulation, no-slip boundary conditions around the membranes are used to incorporate the formation of boundary layers. To decrease the computational complexity, the air is modeled using the acoustic PDE, (8), as quickly as possible.

$$\frac{1}{c^2}\frac{\partial^2 p_{\mathrm{a}}}{\partial t^2} - \Delta p_{\mathrm{a}} = 0 \tag{8}$$

The LinFlow domain is directly coupled to the acoustic domain as soon as the boundary layer is fully developed. The acoustic PDE then models the surrounding air domain, which is finally enclosed by a perfectly matched layer to absorb outgoing waves. A structure of the domains resembling the model given in 2 and the corresponding PDEs is given in Fig. 4.

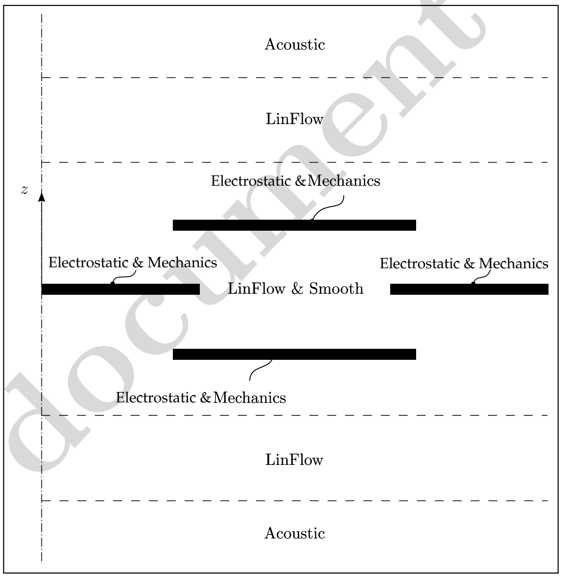

Figure 4: Physical domain structure in the side view of the microspeaker schematic.

Additionally, Fig. 5 depicts the described overall simulation workflow used for the simulation.

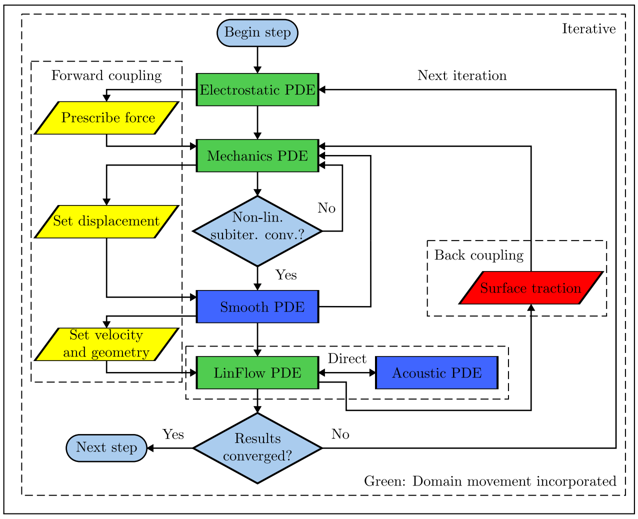

Figure 5: Coupling framework used in *openCFS*.

5. Simulation Results

The simulation results yield the air pressure above the microspeaker for both linear and nonlinear mechanical cases. In both cases, viscous effects in the air channels dominate the modulation. On the one hand, the sealing effect of a closing gap is vital for the redirection of the air stream. On the other hand, viscous effects are responsible for the generation of an air cushion between the membranes (squeeze film). This squeeze film exhibits a damping force that is the main back-coupling force counteracting the electrostatic actuation. Since the importance of viscous effects and their influence on the membrane movement has also been discussed already in the literature [3], the focus of this evaluation is laid upon the power spectral density (PSD) of the audio signal. In the PSDs for both scenarios, the demodulated audio signal components are observed. Furthermore, the presence of harmonic distortion confirms the nonlinear effects induced by viscous effects. For each frequency peak in the power spectral density, the frequency band introduced by the window function used to integrate over the peak to retrieve the total signal power at the specific frequency. Fig. 6 and 7 show the respective power spectral densities. From the identified peaks, the total harmonic

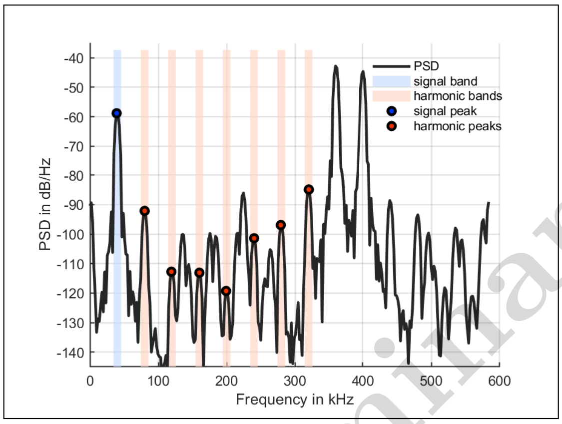

Figure 6: Power spectral density of the simulated air pressure above the microspeaker using linear mechanics simulation. Blue: low-frequency audio signal. Red: harmonic distortions

distortion (THD) is calculated by integrating over the frequency bands. The THD values are given in Table 1

Table 1: Calculated total harmonic distortion from the corresponding power spectral density

	THD in dB
linear	-25.379
nonlinear	-7.777

When non-harmonic distortions are included in the linear mechanics simulation, the total harmonic distortion (THD) increases to −23.231 dB. This minor

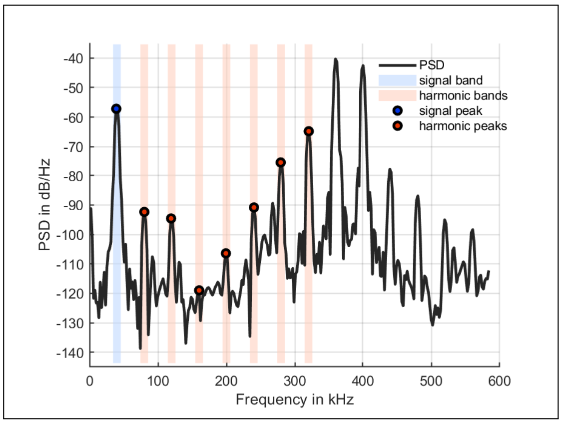

Figure 7: Power spectral density of the simulated air pressure above the microspeaker using non linear mechanics simulation. Blue: low frequency audio signal. Red: harmonic distortions.

increase does not significantly impact the results, as the non-harmonic peaks remain at least 60 dB below the signal. The primary contribution to THD arises as sidebands from the carrier frequency. This contribution is especially pronounced in the power spectral density of the nonlinear simulation, which appears to be underestimated by approximately 20 dB compared to the linear simulation. It appears that the increase stems from the difference frequencies of the modulation and carrier signals from the non-linear mechanics. These difference frequencies are also present, although less attenuated, in the linear mechanics case, as the influence of the non-linear viscous effects also seems to yield those frequencies. For the non-linear mechanics case, both effects superimpose. This yields a far greater difference when including non-linear mechanics as initially expected. It has to be said, though, that for a carrier frequency high enough, the sidebands will not reach the audible frequency range. The reason for this is the sharp decline seen in the PSD in Fig. 7 combined with the fact that the usable audio frequency is capped at 20 kHz. Besides the sidebands of the carrier frequency, also the audio frequency shows higher harmonics that contribute to the THD. These sidebands are in the audible band and should be minimized. This could be either done with design modifications or excitation signal adaptations (pre-distortion). Finally, it has to be noted that since the carrier frequency is a multiple of the audio frequency, the harmonics and sidebands can potentially overlap.

6. Conclusion and outlook

In conclusion, this investigation shows the importance of including nonlinear mechanics when simulating MEMS microspeakers. Using linear mechanics to speed up the simulation not only underestimates harmonic distortion but also introduces non-harmonic components that need further investigation. Relying on these results in the development phase is crucial for predicting system performance and, as we showed in this simple example, underestimating the THD by around 20 dB and adapting the frequency response based on the harmonic distortions is fatal. The power spectral densities also show that the most energy contributing to the harmonic distortion is located at the sidebands of the carrier. In a real audio application, those frequencies would not fall into the audible spectrum. Additionally, higher harmonics of the audio frequency have been observed, which are in the audible range and need to be minimized accordingly. We also showed that a highly coupled finite element simulation can be done using only open-source software, providing a cost-effective and accessible alternative to commercial modeling and meshing tools and FEM solvers. This approach improves reproducibility and transparency within the research community, enabling broader adoption and continuous improvements to the simulation tools used.

References

[1] H. Wang, Y. Ma, Q. Zheng, K. Cao, Y. Lu, and H. Xie, "Review of recent development of mems speakers," *Micromachines*, vol. 12, no. 10, p. 1257, 2021.

[2] D. Mayrhofer, T. Wilczacki, and M. Kaltenbacher, "Simulation of mems speakers using the linearized flow equations with maxwell slip boundary conditions," in *Proceedings of the 50th German Annual Conference on Acoustics (DAGA)*, Stuttgart, Germany, 2024, pp. 1077–1080.

[3] D. Mayrhofer, T. Wilczacki, and M. Kaltenbacher, "Overview and simulation of modulated ultrasound mems loudspeakers," in *Proceedings of the 52nd German Annual Conference on Acoustics (DAGA)*, Dresden, Germany, 2026, pp. 911–914.

[4] S. Chen, M. Harteg, and M. Margalit, "Modulated ultrasound speakers - a common framework for analyzing air pump speakers," *Sensors and Actuators A Physical*, vol. 381, Dec. 2024. DOI: 10.1016/j.sna.2024.116086.

[5] S. Chen and M. Margalit, "Comparative analysis of active modulated ultrasound speaker architectures," *Physica Scripta*, vol. 101, no. 4, p. 045 906, Jan. 2026. DOI: 10.1088/1402-4896/ae3991. [Online]. Available: https://doi.org/10.1088/1402-4896/ae3991.

[6] C. Geuzaine and J.-F. Remacle, "Gmsh: A 3-d finite element mesh generator with built-in pre- and post-processing facilities," *International Journal for Numerical Methods in Engineering*, vol. 79, no. 11, pp. 1309–1331, 2009. DOI: 10.1002/nme.2579.

[7] M. Kaltenbacher, *openCFS*, https://www.opencfs.org, version 26.01, 2026.

[8] D. Mayrhofer, K. Roppert, D. Tumpold, and M. Kaltenbacher, "A moving mesh method for fluid-solid-acoustic interactions in mems devices," English, *Journal of Theoretical and Computational Acoustics*, vol. 32, no. 4, Dec. 2024. DOI: 10.1142/S2591728524500166.